PROCESS ZONE LENGTH AND FRACTURE ENERGY OF SPRUCE WOOD IN MODE-I FROM SIZE EFFECT

*Simon Aicher**†

Academic Director
Division of Timber Construction
Materials Testing Institute (MPA)
University of Stuttgart
Pfaffenwaldring 4
70569 Stuttgart, Germany

(Received November 2009)

Abstract. This article reports on the determination of fracture energy and fracture process zone length in Mode I fracture of European spruce wood loaded in tension perpendicular to the fiber direction based on Bazant's size effect law. Within the size effect model, fracture energy and fracture process zone length are correlated and represent unambiguous limit values for large structures or specimens. The model parameters were derived from an earlier experimental size effect study on specific single-edge notched beam specimens with a scale range of 1:32. The Mode I fracture energy range of 250-290 N/m, derived from the size effect law, is in agreement with fracture energies obtained for the same specimens based on external work to complete specimen failure. The elastically equivalent length of the fully developed fracture process zone ahead of the nominal crack tip was determined to be in the range of about 2 mm. The stated independent proof of the correlated fracture energy confirms the validity of the derived size of the fracture process zone. Furthermore, fracture process zone size obtained is in close agreement with a previous result for eastern Canadian spruce, a finding based on scanning electron microscopy.

Keywords: Fracture, fracture energy, Mode I, size effect, process zone, spruce, wood.

INTRODUCTION

In timber engineering and wood drying, the Mode I fracture with a crack parallel to longitudinal (L) fiber direction in solid wood or glulam, initiated and driven by tension stresses perpendicular to fiber direction bound to mechanical and/or moisture loads, is of great importance. This is especially true for splitting failures in curved and pitched cambered glulam beams or in timber joints with dowel-type fasteners. The orientation of the normal vector of the crack plane, resulting from loading perpendicular to fiber direction, may conform to the limit cases of pure radial (R) or tangential (T) direction and in general is at some angle between R and T directions. The respective Mode I fracture planes are then denoted by RL, TL, and (R/T)L.

The material parameters, fracture energy, and fracture process zone length are decisive for the characterization and modeling of the fracture process and the material resistance to crack initiation and propagation. In a perfectly brittle material containing a crack, all of the fracture process at tension and/or shear loading takes place at the crack tip. In many common materials, including wood, the fracture process is not confined to a point but occurs within a certain length (area), termed fracture process zone, stretching out ahead of the crack tip. Depending on the respective material, hardening, ideal plastic behavior, or softening may occur in the process zone. Hardening and plasticity are features demonstrated by most metals (Dugdale 1960), whereas softening is typical, ie for concrete (Hillerborg et al 1976; Reinhardt 1984) and for wood (Boström 1992) when loaded in tension perpendicular to the fiber direction. In all cases, additional energy is dissipated in the fracture process zone during progressive damage as compared with ideal brittle fracture, thus increasing the energetic fracture resistance, termed fracture energy. In

* Corresponding author: simon.aicher@mpa.uni-stuttgart.de
† SWST member

the softening of wood, damage mechanisms like slipping, friction, decohesion, and pullout of the gap-bridging fibers (Vasic and Smith 2002; Vasic et al 2002) and effects of anisotropy and material inhomogeneity (Dill-Langer et al 2000; Landis et al 2002; Dill-Langer 2004) contribute to the nonlinear fracture resistance. The described energy dissipation and degradation evolution increases the required energy input, termed strain energy release rate, to drive the fracture process.

In this article, both fracture energy and fracture process zone length or, more precise, the elastically equivalent size of the fracture process zone are consistently derived by Bazant's nonlinear size effect law (Bazant 1984; Bazant and Pfeiffer 1987) by re-evaluating the results of an earlier study (Aicher et al 1993) on the influence of size on tension strength perpendicular to grain in notched beam specimens of European spruce.

LITERATURE REVIEW

Fracture energy can be determined through stable crack growth tests by evaluating the external work to create new unit areas of crack surfaces. The experiments may be performed with monotonic loading until complete specimen failure with separation of the crack surfaces or by successive loading and unloading with associated crack elongation measurements. Determination of fracture energy in Mode I loading perpendicular to fiber direction has been primarily conducted on single-edge notched beams (SENB) or through wedge splitting test arrangements on several wood species, including spruce, pine, and oak (Larsen and Gustafsson 1989, 1990; Aicher 1994; Smith and Chui 1994; Stanzl-Tschegg et al 1995; Reiterer et al 2000).

However, with regard to fracture process zone size quantification, there are very few investigations reported in the literature. An experimental micromechanical study on the characterization and size of the fracture process zone in eastern Canadian spruce was performed by Vasic et al (2002) by means of in situ real-time scanning electron microscopy (SEM). According to this investigation, after initiation, the crack grows in a highly localized manner with a length of the fracture zone of about 1-2 mm. No evidence was found for a larger zone of microcracks ahead of the crack tip as seen for example in concrete or ceramics. Computations using a distinct bridging crack model (BCM), which contrary to usual cohesive crack models is based on the assumption of coexistence of a sharp crack tip and a nonfictitious bridging zone behind it, resulted in a bridging zone length of 4 mm for Canadian spruce (Vasic and Smith 2002; Smith et al 2003). The stated bridging zone size coincides with the fiber length of eastern Canadian spruce.

Apart from the cited experimental determinations of fracture energy and process zone length and the semicomputational BCM model approach, a further method, based on Bazant's nonlinear size effect law, appears possible. The approach that has been successfully applied to rock, concrete, and other cementitious materials (Bazant 1984, 1987; Bazant and Pfeiffer 1987; Bazant and Kazemi 1990; N N 1990) enables the consistent determination of both fracture energy and elastically equivalent process zone length as interdependent material properties within the frame of a one-model assumption. Although the size effect model has been applied in earlier studies on the evaluation of strength vs size relationships of Mode I and II fractures in spruce, pine, and oak (Aicher 1992; Aicher et al 1993; Morel and Valentin 1996), the literature so far provides no evidence of a successful application of Bazant's size effect concept to fracture energy and process zone determination in wood fracture.

UNAMBIGUOUS DEFINITION OF FRACTURE ENERGY

For an ideal brittle material, fracture energy (G_f) is a constant, often termed critical energy release rate (G_c). On the contrary, in cases of materials exhibiting softening, G_f is a function of crack extension c and of the characteristic specimen size d, ie $G_f = R_{(c,d)}$. Figure 1a illustrates the fact, well proven by experiments, that for softening materials, the resistance to crack propagation, termed R-curve, increases

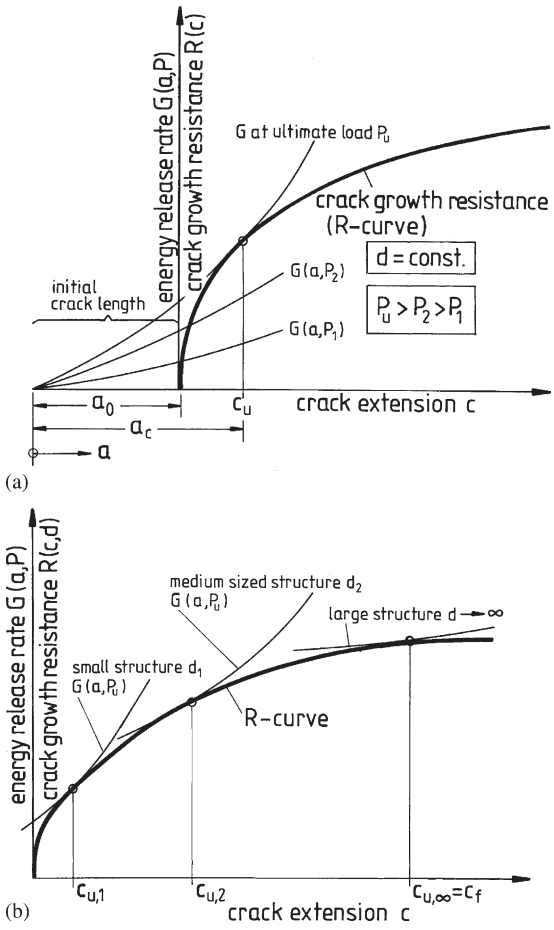

Figure 1. General relationship of crack growth resistance (R-curve) and crack extension of fracture softening materials. (a) Unique size; (b) similar structures of different sizes.

with growing extension c of an initial crack of length $a = a_0$. Quantity c may be regarded as the elastically equivalent length of the fracture process zone with gradually decreasing capability to sustain transverse tension or shear stresses in case of Mode I and II crack loading, respectively.

For a given specimen size d and an initial notch length a_0, fracture at ultimate load P_u occurs when crack extension c has grown during loading to its specimen size-dependent maximum length $c = c_u(d)$, thus determining the critical crack length $a_u = a_0 + c$. In the postpeak regime, ie beyond the ultimate load on the descending load deformation path—stable fracture assumed—the length of the fully developed process zone $c = c_u$ may be assumed to be roughly constant. The parametric dependency of process zone length respective of its elastically equivalent length c vs specimen size d is depicted in Fig 1b. The graph shows that the process zone length c is related to specimen or crack size in such a manner that c is a degressively increasing function of d, reaching a limit value c_f altogether with an asymptotic value for the energetic fracture resistance R(c,d) at very large specimen sizes $d \rightarrow \infty$. It is important to mention that the experimentally measured R-curve depends considerably on the shape of the structure and is valid only for specimens of similar geometry (Bazant and Cedolin 1991; Morel et al 2003).

Based on this discussion of fracture energy and process zone as influenced by the absolute size of the structure/specimen, the material properties G_f and c_f are unambiguously defined as the energy required for crack growth and the related length of the elastically equivalent fracture process zone in an infinitely large structure (Bazant 1987; Bazant and Cedolin 1991). This definition can be written mathematically as

$$G_f = \lim_{d\to\infty} R(c, d) \quad \textit{and} \quad c_f = \lim_{d\to\infty} c(d) \tag{1a-b}$$

Contrary to the stated limitations of R-curves as being dependent on specimen shape, the given definitions of fracture energy and fracture process zone are independent of specimen size and shape and hence provide intrinsic material properties. With regard to the pretentious term "intrinsic," it should be born in mind that this statement refers—like with all engineering material properties—to a global, ie smeared, material characteristic within the frame of nonlocal fracture mechanics.

BAZANT'S NONLINEAR SIZE EFFECT LAW

Basic Equations for Size Law, Fracture Energy, and Process Zone Length

The equation of the used nonlinear size effect law (Bazant 1987; Bazant and Cedolin 1991)

and its relation to fracture energy and process zone length is concisely given in the following with consideration to the anisotropic behavior of the material wood. As a result of the defined limit character of G_f and c_f, in an approximation for the ultimate load state of a structure of size d, the proportionality condition of energy release rate and fracture energy can be written as

$$\frac{G\ (\alpha,\ P_u)}{g\ (\alpha)} = \frac{G_f}{g\ (\alpha_f)} \qquad (2)$$

where

$$G\ (\alpha,\ P_u)\ =\ g\ (\alpha)\ \ \frac{P_u^2}{d\ b^2\ E_{eff}} \qquad (3)$$

with

$$\alpha\ =\ \frac{a}{d} = \frac{a_0\ +\ c}{d}\ =\ \alpha_0\ +\ \frac{c}{d} \qquad (4)$$

and

$$g\ (\alpha_f)\ =\ g\ (\alpha_o)\ +\ g'\ (\alpha_0)\ \frac{c_f}{d} \qquad (5)$$

where

$$\alpha_f = \alpha_0\ +\ \frac{c_f}{d},\ \ g'(\alpha_0) = \frac{d\,g\ (\alpha_0)}{d\,\alpha} \qquad (6,7)$$

$$E_{eff}\ =\ \sqrt{2\,E_x\,E_y}\ \left[\sqrt{\frac{E_x}{E_y}}\ +\ \frac{E_x}{2\ G_{xy}} - \nu_{yx}\right]^{-0.5}$$

$$whereby\ \nu_{yx} = \nu_{xy}\,E_x/\,E_y \qquad (8a\text{-}b)$$

Term $G(\alpha, P_u)$ is the (strain) energy release rate $G = G(\alpha, P)$ at maximum load $P = P_u$, which is related to a specific crack extension c (here: parallel to the x-axis) of a given structure with characteristic size d (here: parallel to the y-axis), width b, and effective modulus of elasticity E_{eff} (see subsequently). $g(\alpha)$ represents the normalized energy release rate, ie a shape function depending on the specimen shape including the normalized crack extension c/d. Quantity α is the size-normalized full length a of the elastically equivalent crack. Expression $g\ (\alpha_f) = g\ (\alpha_0 + c_f/d)$ is the normalized energy release rate with regard to the limit value of crack extension $c = c_f$. Quantity E_{eff} represents the effective modulus of elasticity, which conforms to Young's modulus in cases of isotropic material and plane stress conditions. In the case of an orthotropic material like wood, assuming plane stress conditions and crack extension parallel to wood fiber direction (x-axis), E_{eff} is defined (Sih et al 1965) according to Eqs 8a-b.

Substituting $G\ (\alpha, P_u)$ and $g\ (\alpha_f)$ in Eq 2 by Eqs 3 and 5 delivers for an ultimate load

$$P_u\ =\ \sqrt{\frac{G_f\ E_{eff}\ b^2\ d}{g\ (\alpha_0)\ +\ g'\ (\alpha_0)\ \cdot\ \left(c_f/d\right)}} \qquad (9)$$

Substitution of ultimate load P_u in Eq 9 by nominal strength (factor c_n depends on the respective test configuration)

$$\sigma_N\ =\ \frac{P_u\ c_n}{b\ d} \qquad (10)$$

yields the nonlinear size effect law, ie the relation between nominal strength and the characteristic structure or specimen size d

$$\sigma_N\ =\ \frac{B}{\sqrt{1\ +\ d\ /\ D_0}} \qquad (11)$$

where

$$B\ =\ \sqrt{\frac{G_f\,E_{eff}\,c_n^2}{g'\ (\alpha_0)\ c_f}}\ \ \ and\ \ \ D_0\ =\ \frac{g'(\alpha_0)\ c_f}{g\ (\alpha_0)}. \qquad (12a\text{-}b)$$

DETERMINATION OF SIZE EFFECT LAW PARAMETERS BY LINEAR TRANSFORMATION

The parameters B und D_0, defining the size dependency of nominal strength σ_N, can be derived empirically by means of tests performed with geometrically similar specimens of significantly different sizes. Parameter determination can be achieved by transforming the size effect expression (Eq 11) into an equivalent linear format

$$Y\ =\ C + d\,A \qquad (13)$$

where

$$Y = \frac{1}{\sigma_N^2}, \quad C = \frac{1}{B^2} \quad \textit{and} \quad A = \frac{1}{B^2 D_0} = \frac{C}{D_0}. \tag{14a-c}$$

The parameters C and A of the linear substitution (Eq 13) can now be obtained from a linear regression approximation of the experimental data of a size effect study, hence delivering B and D_0 through Eqs 14b-c. Additionally, the elastically equivalent fracture process zone length c_f and fracture energy G_f can be derived by introducing B and D_0 in Eqs 12a-b.

SIZE EFFECT LAW PARAMETERS FOR SPRUCE

Test Scheme and Specimen Geometry and Sizes

With regard to experimental data, this article relies on results from an earlier investigation on the nonlinear fracture behavior and the related size effect of clear wood of European spruce (*picea abies*) loaded in tension perpendicular to the fiber direction (Aicher et al 1993). The tests were performed with a specific type of SENB specimen (Larsen and Gustafsson 1990) that was designed for direct experimental determination of fracture energy.

The beam specimens consisted of three parts with two different orientations of fiber direction; these were glued together as shown in Fig 2. The actual test volume with fiber direction parallel to beam depth d was located at midspan. Adherents with fiber direction parallel to beam axis were glued to both vertical narrow side faces of the test volume. The test volume incorporated a single edge notch at the bending tension side with a rather long initial notch length of $a_0 = 0.6$ d to assure stable crack propagation. For the size effect study presented here, only the maximum loads before softening were evaluated. The longitudinal–tangential growth plane of the test volume and hence of the initial notch plane were—throughout—approximately normal to the beam axis (see Fig 2). Thus, the obtained size effect parameters apply to the so-called RL crack configuration.

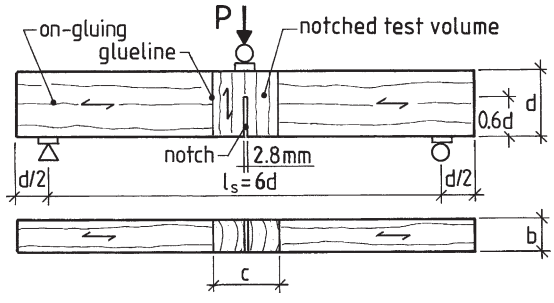

Figure 2. Specimen geometry and test scheme of single-edge notched beam (SENB) specimen used in the Mode I size effect study.

The size range of the geometrically (2D) similar specimens covered beam depths d of 10, 20, 40, 80, 160, and 320 mm; beam width throughout was b = 44 mm. The shape of the test volumes within the beam plane was quadratic, except for depths d of 160 and 320 mm where—material bound—the length c of the test volumes in beam length direction was 0.5 and 0.25 d, respectively. Each sample set, with specimens of the same size, consisted of 16 specimens with the exception of the sample with d = 320 mm in which only 5 specimens were investigated. Nonetheless, it is noteworthy that exclusion of the specific sample has no impact on the derived size effect results. All test volumes, cut from two boards of European spruce, were straight-grained and showed no macroscopic defects. Before the gluing of the SENB assembly, the test volumes were conditioned to moisture equilibrium in a constant climate of 20°C and 65% RH; the mean values for density, annual ring width, and moisture content (MC) were $\rho_{12} = 460 \pm 24$ kg/m^3, r = 2.5 mm, and u = 11.8%, respectively. The specified MC also refers to the state of testing.

The three-point bending tests with a midspan load and a span-to-depth ratio of $l_s/d = 6$ were performed in displacement control with a constant rate of cross-head speed per specimen size ranging from 0.4 mm/min for d = 10 and 20 mm to 0.8 mm/min at d = 320 mm. The given loading rates resulted in times to maximum load of about 2 min and complete failure of the specimen was

attained within 6-10 min depending on specimen size. The conditions in the test room were about 20°C and 55% RH.

TEST RESULTS AND SIZE EFFECT LAW

Figure 3a shows the individual bending test results in the format of nominal strength $\sigma_N = 9\ P_u/(b\ d)$ vs beam depth d. Furthermore, a least-squares fitted power function $\sigma_N = a \cdot d^b$ is given, whose parameters were determined as $a = 3.71\ MN/m^2$ and $b = -0.408$ (note: d in mm, non-dimensional). The graph also shows the shape parameter, ie the exponent m of a 2-parameter Weibull (cumulative) strength distribution function $(1\text{-}\exp[-\{\sigma_N/\sigma_0\}^m])$ for each sample with specific size d. The scatter of the shape parameters varies from 6.6-8.8, thus being rather similar for all investigated sizes (for details including values for the scale parameter σ_0, see Aicher et al 1993). Figure 3b presents the primary test results transformed into a linear relationship of σ_N^{-2} and d (in mm) according to Eq 13. The linear approximation of the transformed test results yields the regression parameters

$$A = 26.54 \left[\frac{m^3}{MN^2}\right], \quad C = 0.4242 \left[\frac{m^4}{MN^2}\right].$$

From the linear regression parameters A and C, one obtains the size effect law coefficients via Eqs 14b-c

$$B = 1.535 \left[\frac{MN}{m^2}\right], \quad D_0 = 16.0\ [mm].$$

Figure 4 depicts the nonlinear size effect relationship between nominal strength σ_N and characteristic size d given in Figs 3a-b, now expressed by the size effect law (Eq 11), using the derived previously stated coefficients B and D_0. In detail, the size effect relationship is presented in double logarithmic scaling, ie lg σ_N vs lg d. The chosen logarithmic representation enables clear visualization of the fact that the size effect law equation inherently describes the transition from fracture behavior according to linear elastic fracture mechanics for large sizes $d \to \infty$ (range with linear slope of –0.5) to a conventional strength of materials approach for very small sizes $d \to 0$ in which strength, on the macroscopic scale, can be considered a scalar quantity (here: $\sigma_N = B$). This is shown to also be very suitable for application in investigations of wood in Mode I fracture with tension loading perpendicular to fiber direction.

LENGTH OF ELASTICALLY EQUIVALENT FRACTURE PROCESS ZONE

The determination of the length of the fully developed elastically equivalent fracture process zone $c = c_f$ from Eqs 12a-b necessitates the determination of the normalized strain energy $g(\alpha)$ as a steadily differentiable function of normalized crack length α. Here, function $g(\alpha)$ was derived from an analytical solution for Mode I stress intensity factor K_I and its respective stress intensity shape function $f(\alpha)$ for a three-point bending specimen with a single-edge center notch (Brown and Srawley 1966)

$$K_I = \frac{6\,M\sqrt{a}}{b\,d^2}\ Y(\alpha) \qquad (15a)$$

where

$$Y(\alpha) = A_0 + A_1\,\alpha + A_2\,\alpha^2 + A_3\,\alpha^3 + A_4\,\alpha^4 \qquad (15b)$$

(Note: see subsequently for explicit values of parameters A_0 to A_4 depending on the span-to-depth ratio.) To obtain a different format for Eq 15a, moment M is replaced by load P (see Eq 10) and section modulus $S = bd^2/6$ yielding

$$M = \frac{P\,c_n}{b\,d} \quad \cdot \quad S = \frac{P\,c_n\,d}{6} \qquad (16)$$

Now, the Mode I stress intensity factor according to Eq 15a can be rewritten as

$$K_I = \frac{P}{b\sqrt{d}}\,k(\alpha) \quad where \quad k(\alpha) = c_n\sqrt{\alpha}\ Y(\alpha) \qquad (17a\text{-}b)$$

The experimental size effect study had been performed, as mentioned, with a span-to-depth ratio of $s/d = 6$. For this s/d ratio, the shape function

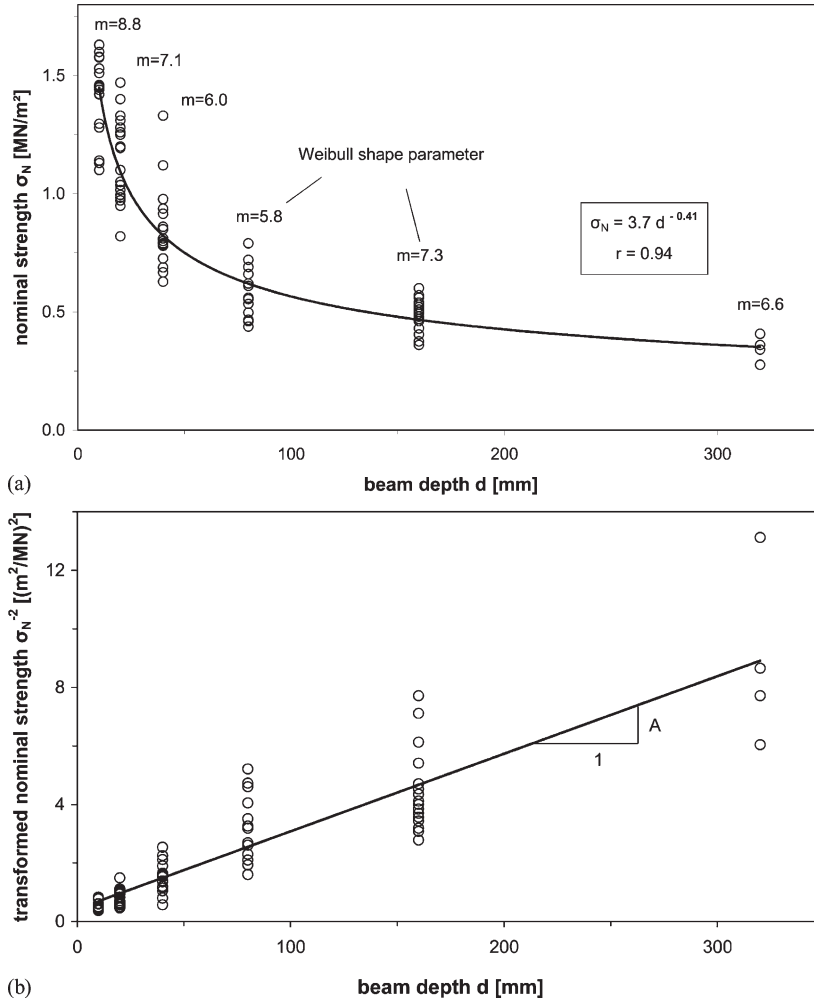

Figure 3. Nominal bending strengths σ_N depending on beam depths d of investigated 2D geometrically similar specimens. (a) σ_N vs d; (b) transformed results σ_N^{-2} vs d.

parameters A_0 to A_4 in Eqs 15b and 17b were determined as

$$A_0 = 1.945, A_1 = -2.91, A_2 = 14.095,$$
$$A_3 = -24.545, A_4 = 25.51$$

based on a linear interpolation of the parameters A_i for s/d = 4 and s/d = 8 as specified by Brown and Srawley (1966) for beams of isotropic material. With regard to the actual orthotropic constitutive law of the test volumes and the heterogeneous build-up of the specimens, finite element analysis was used to verify that the parameters also apply in close approximation to the used specimens. Parameter c_n in Eq 17b becomes $c_n = 9$ for the specific load configuration and span-to-depth ratio of 6 when replacing M in Eq 16 by 3Pd/2.

Through reference to the general relationship between energy release rate and stress intensity factor

$$G = \frac{K^2}{E_{eff}} \tag{18}$$

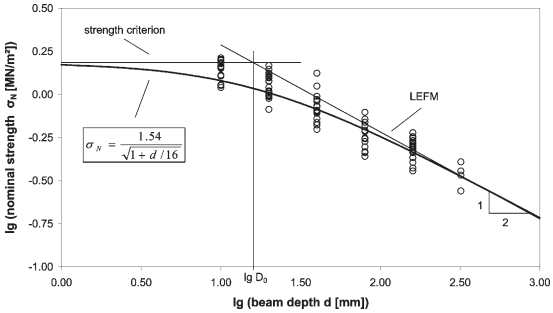

Figure 4. Empiric relationship between nominal bending strengths and beam depths, expressed by lg σ_N vs lg d, and approximation of the test results by Bazant's nonlinear size effect law.

the relation between normalized strain energy $g(\alpha)$ and normalized stress intensity $k(\alpha)$ is obtained by inserting Eqs 3 and 17a in Eq 18, resulting in

$$g(\alpha) = k^2(\alpha) \tag{19}$$

Using the previously specified values for A_0-A_4 and c_n yields for normalized strain energy

$$g(\alpha) = (17.51\alpha^{0.5} - 26.19\alpha^{1.5} + 126.86\alpha^{2.5} - 220.91\alpha^{3.5} + 229.59\alpha^{4.5})^2 \tag{20}$$

For determination of the elastically equivalent length of the fracture process zone, c_f, normalized strain energy release rate and its first derivative have to be evaluated for the actual initial notch to beam depth ratio $\alpha = \alpha_0 = 0.6$, giving

$$g(\alpha = 0.6) = 522.3\,[-] \text{ and}$$
$$g'(\alpha = 0.6) = 3909\,[-]$$

Quantity c_f can now be calculated from Eq 12b using the previously stated values for D_0, $g(0.6)$ and $g'(0.6)$ as

$$c_f = 2.14\,\text{mm}.$$

The derived magnitude of the elastically equivalent process zone length is roughly 30-50% of the length of European spruce tracheid cells, which have a range of about 4-6 mm. The obtained fracture process zone size conforms well to SEM results by Vasic et al (2002) for eastern Canadian spruce. A further confirmation of the given result for the process zone length stems from the direct proportionality of c_f and G_f (see Eqs 12a and 21a) as G_f based on the size effect approach is also validated by an independent, fully experimental method (see subsequently).

FRACTURE ENERGY G_F

Fracture energy G_f can be directly determined from Eq 12a thereby revealing the direct relation with fracture process zone length

$$G_f = c_f \frac{g'(\alpha_0)}{E_{eff}} \left(\frac{B}{c_n}\right)^2 \tag{21a}$$

Eq 21a can be rewritten in a more comprehensive manner by substituting c_f and B through expressions 12b and 14c, giving

$$G_f = \frac{g(\alpha_0)}{A} \cdot \frac{1}{E_{eff}\, c_n^2} \tag{21b}$$

Eq 21b reveals that fracture energy is fully determined by normalized strain energy for initial notch-to-depth ratio α_0 and by the slope A of the linearized size effect relationship (Eq 13); effective modulus of elasticity E_{eff} and the system factor c_n are constants.

Instead of the previously stated formal derivation of fracture energy, the limit character of G_f becomes more evident making use of the basic definition (Eq 1a), which by means of Eq 3 and the failure criterion $G(\alpha, P_u) = R(c,d)$ can be expressed as

$$G_f = \lim_{d\to\infty} R(c, d) = \lim_{d\to\infty} \frac{g(\alpha)\, P_u^2}{d\, b^2\, E_{eff}}. \tag{22a}$$

Replacing $P_u = \sigma_N\, b\, d/c_n$ by the size effect law Eqs 11 and 12a, b then gives rise to

$$G_f = \lim_{d\to\infty} \frac{B^2\, d\, g(\alpha)}{E_{eff}\, c_n^2\, (1 + d/D_0)} \tag{22b}$$

Considering the limit case of very large structures or specimens, ie $d \to \infty$, leads to

$c = c_f \ll d$, therefore $\alpha = \alpha_0 + c_f/d \approx \alpha_0$ and $\lim_{d\to\infty} g(\alpha) = g(\alpha_0)$.

Eq 22b can then be written as

$$G_f = \frac{B^2 g(\alpha_0)}{E_{eff}\, c_n^2} \lim_{d\to\infty} \frac{d}{1 + d/D_0} \qquad (22c)$$

which is as a consequence identical to Eq 21b considering $\lim_{d\to\infty} \frac{d}{1 + d/D_0} = D_0$ and Eq 14c. To determine G_f from Eqs 21a or 21b, the effective modulus of elasticity E_{eff} according to Eqs 8a-b has to be known. With regard thereto, it has to be mentioned that the four independent elasticity coefficients E_x, E_y, G_{xy}, ν_{yx} (x, y = parallel and perpendicular to fiber direction) defining E_{eff} have not been measured in the herein described experimental size effect investigation on clear spruce wood. Irrespective thereof, realistic ranges of the relevant stiffness parameters can be assessed by using the elasticity ratios $E_x/E_y = 30$, $E_x/G_{xy} = 16$ as stated implicitly in the European standard EN 338 on strength classes for softwoods. The Poisson ratio ν_{yx}, as defined by Eq 8b, can be assumed to be 0.45 (Aicher et al 1995). Based on the given elasticity and Poisson ratios, Eq 8a results in $E_{eff} = E_x/14$ for the effective modulus of elasticity, depending exclusively on Young's modulus E_x parallel to fiber direction.

The elasticity value E_x parallel to fiber of the investigated specimens, according to the given values for density and annual ring width, can be assumed to be in the range of about 12,000-14,000 MN/m^2 and hence E_{eff} = 850-1000 MN/m^2. By inserting this range for E_{eff} in Eq 21b together with quantities A = 26.5 [m^3/MN^2], g (0,6) = 522 [–], and $c_n = 9$, one obtains for fracture energy a range of

$$G_f \approx 240\text{-}290\ \mathrm{N/m}.$$

The derived semiempiric result for the asymptotic unambiguous limit value of fracture energy G_f, based on the size effect law assumptions, is highly consistent with fracture energies determined for the same specimens in an alternative approach based on total external work (Aicher 1994), where the empiric fracture energy median (3-parameter Weibull fit) was 276 N/m. This result agrees well with results for spruce given by Larsen and Gustafsson (1990) in which G_f = 285 N/m for ρ = 460 kg/m^3. Reiterer et al (2000) state a G_f value of 260 N/m without density specification. Moreover, the insertion of the previously given total work G_f median into Eq 21b produces an effective modulus of elasticity of E_{eff} = 900 MN/m^2, which substantiates the stated stiffness assumptions.

SUMMARY AND CONCLUSIONS

Bazant's nonlinear size effect law enables the derivation of the directly related quantities fracture process zone length and fracture energy. In the case of wood, however, the model, so far, had been primarily used for a theory-based approximation of strength data from size effect studies. In this article, a previously known size effect study on Mode I fracture of European spruce subjected to tension perpendicular to fiber and crack propagation parallel to fiber was re-evaluated with regard to fracture energy and fracture process zone length.

Based on the derived size effect law parameters, the resulting length of the fracture process zone was 2.1 mm. This value is highly consistent with previously reported results that were obtained from in situ fracture observations on eastern Canadian spruce by means of SEM. The limit value of fracture energy derived from the size effect law was in the range of 240-290 N/m. This model-based result comprises the median of the directly measured fracture energies based on external work, 276 N/m. Because of the direct correlation of fracture energy and fracture process zone length in the frame of Bazant's size effect model, the independent proof of the fracture energies also supports the derived size of the process zone length.

In conclusion, it can be stated that the nonlinear effects, increasing the energetic fracture resistance of spruce wood subjected to tension perpendicular to fiber direction and crack propagation parallel to fiber, are confined to a very small region of about

one-half of the fiber length ahead of the nominal crack tip. This result is very different from that of most cementitious materials.

It has to be mentioned that the findings are related to European spruce with a MC of about 12% and a temperature of about 20°C. As for the influence of MC, the literature gives evidence of a pronounced decrease of fracture energy with reduction of MC within in the range of 8-18% (Smith and Chui 1994). Contrary to this, Petterson and Bodig (1983) have shown a steady increase of fracture toughness with decreasing MC. It is therefore reasonable to assume that the different moisture sensitivities of both fracture mechanics parameters are related to the moisture-dependent micromechanical damage mechanisms in the fracture process zone. This could have an impact on its size as well. Because temperature shows a pronounced effect on fracture energy and toughness (Reiterer 2001), the fracture process zone dimensions could be influential. With regard to generalization of the presented results, it seems worthwhile to reveal the potential influences of moisture and temperature as well as the effect of wood species and fracture plane configurations.

In a general sense, this investigation emphasizes the fact that in the specific RL cracking configuration—which is very relevant for timber structures—spruce, despite some evident material softening, displays highly brittle behavior.

REFERENCES

Aicher S (1992) Fracture and size effect law for spruce and oak in mode I and mixed mode I and II. Proc RILEM TC 133 Meeting, LRBB, Bordeaux, France.

Aicher S (1994) Fracture energy, critical strain energy release rate and fracture toughness of spruce in tension perpendicular to grain. Holz Roh Werkst 52(6):361-370 [in German].

Aicher S, Reinhardt HW, Klöck W (1993) Non linear fracture mechanics size effect law for spruce in tension perpendicular to grain. Holz Roh Werkst 51(6):385-394 [in German].

Aicher S, Schmidt J, Brunold S (1995) Design of timber beams with holes by means of fracture mechanics. Paper 28-19-4 *in* Proc CIB W18 Meeting 28; Copenhagen, Denmark.

Bazant ZP (1984) Size effect in blunt fracture: Concrete, rock, metal. J Eng Mech 110:518-525.

Bazant ZP (1987) Fracture energy of heterogeneous materials and similitude. Pages 390-402 *in* Proc SEM-RILEM Int Conf on Fracture of Concrete and Rock; Houston, TX.

Bazant ZP, Cedolin L (1991) Stability of structures: Elastic, inelastic, fracture and damage theories. Oxford University Press, New York, NY.

Bazant ZP, Kazemi MT (1990) Determination of fracture energy, process zone length and brittleness number from size effect, with application to rock and concrete. Int J Fract 44:111-131.

Bazant ZP, Pfeiffer PA (1987) Determination of fracture energy from size effect and brittleness number. ACI Materials Journal Nov-Dec:463-480.

Boström L (1992) Method for determination of the softening behaviour of wood and the applicability of a nonlinear fracture mechanics model. PhD Thesis, Report TVBM-1012, Lund University, Lund, Sweden.

Brown WF, Srawley JE (1966) Plane strain crack toughness testing of high strength metallic materials. ASTM STP 410, American Society for Testing and Materials, Philadelphia, PA.

Dill-Langer G (2004) Schädigung von Brettschichtholz bei Zugbeanspruchung rechtwinklig zur Faserrichtung. PhD Thesis, Materials Testing Institute, University Stuttgart, Stuttgart, Germany [in German].

Dill-Langer G, Lütze S, Aicher S (2000) Microfracture in wood monitored by confocal laser scanning microscopy. Wood Sci Technol 36:487-499.

Dugdale DS (1960) Yielding of steel sheets containing slits. J Mech Phys Solids 8:100-108.

Hillerborg A, Modéer M, Petersson PE (1976) Analysis of crack formation and crack growth in concrete by means of fracture mechanics and finite elements. Cement Concr Res 6(6):773-782.

Landis EN, Vasic S, David WG, Parrod P (2002) Coupled experiments and simulations of microstructural damage in wood. Exp Mech 42(4):389-394.

Larsen HJ, Gustafsson PJ (1989) Design of endnotched beams. Paper 22-10-1 *in* Proc CIB W18 Meeting 22, Vol. II; Berlin, Germany.

Larsen HJ, Gustafsson PJ (1990) The fracture energy of wood in tension perpendicular to the grain—results from a joint testing project. Paper 23-10-12 *in* Proc CIB W18 Meeting 23; Lisbon, Portugal.

Morel S, Mourot G, Schmittbuhl J (2003) Influence of the specimen geometry on R-curve behaviour and roughening of fracture surfaces. Int J Fract 121(1-2): 23-42.

Morel S, Valentin G (1996) Size effect in crack shear strength of wood. J. de Physique IV Colloque C6(Suppl): C6-385-C6-393.

N N (1990) Size-effect method for determining fracture energy and process zone size of concrete. RILEM draft recommendations. Mater Struct 23:461-465.

Petterson RW, Bodig J (1983) Prediction of fracture toughness of conifers. Wood Fiber Sci 15(4):302-316.

Reinhardt HW (1984) Fracture mechanics of an elastic softening material like concrete. Heron 29(2):1-42.

Reiterer A (2001) The influence of temperature on the mode I fracture behaviour of wood. J Mater Sci Lett 20:1905-1907.

Reiterer A, Stanzl-Tschegg SE, Tschegg EK (2000) Mode I fracture and acoustic emission of softwood and hardwood. Wood Sci Technol 34(5):417-430.

Sih GC, Paris PC, Irwin GR (1965) On cracks in rectilinearly anisotropic bodies. Int J Fracture Mech 1:189-203.

Smith I, Chui YH (1994) Factors affecting mode I fracture energy of plantation-grown red pine. Wood Sci Technol 28(2):147-157.

Smith I, Landis E, Gong M (2003) Fracture and fatigue in wood. John Wiley & Sons Ltd, Chichester, UK.

Stanzl-Tschegg SE, Tan DM, Tschegg EK (1995) New splitting method for wood fracture characterisation. Wood Sci Technol 29(1):31-50.

Vasic S, Smith I (2002) Bridging crack model for fracture of spruce. Eng Fract Mech 69:745-760.

Vasic S, Smith I, Landis E (2002) Fracture zone characterization—Micro-mechanical study. Wood Fiber Sci 34(1):42-56.